

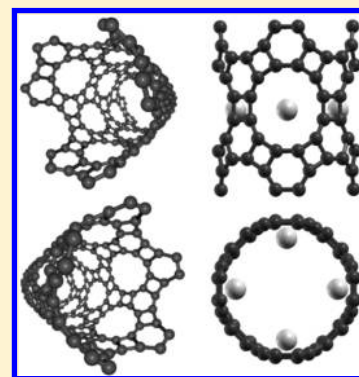
## Graphenylene Nanotubes

Andrew T. Koch,<sup>†</sup> Amir H. Khoshaman,<sup>†</sup> Harrison D. E. Fan,<sup>†</sup> George A. Sawatzky,<sup>‡</sup> and Alireza Nojeh<sup>\*,†</sup>

<sup>†</sup>Department of Electrical and Computer Engineering, University of British Columbia, Vancouver, British Columbia V6T 1Z4, Canada

<sup>‡</sup>Department of Physics and Astronomy, and Department of Chemistry, University of British Columbia, Vancouver, British Columbia V6T 1Z4, Canada

**ABSTRACT:** A new type of carbon nanotube, based on the graphenylene motif, is investigated using density functional and tight-binding methods. Analogous to conventional graphene-based nanotubes, a two-dimensional graphenylene sheet can be “rolled” into a seamless cylinder in armchair, zigzag, or chiral orientations. The resulting nanotube can be described using the familiar  $(n,m)$  nomenclature and possesses 4-, 6-, and 12-membered rings, with three distinct bond lengths, indicating a nonuniform distribution of the electron density. The dodecagonal rings form pores, 3.3 Å in diameter in graphenylene, which become saddle-shaped paraboloids in smaller-diameter nanotubes. Density functional theory predicts zigzag nanotubes to be small-band gap semiconductors, with a generally decreasing band gap as the diameter increases. Interestingly, the calculations predict metallic characteristics for armchair nanotubes with small diameters (<2 nm), and small-band gap semiconducting characteristics for larger-diameter ones. Graphenylene nanotubes with indices  $\text{mod}(n-m,3) = 0$  exhibit a band gap approximately equal to that of armchair graphenylene nanotubes with comparable diameter.



Carbon nanotubes (CNTs) have undergone intense investigation due to their vast array of exciting properties. A CNT can be considered conceptually as a two-dimensional (2D) sheet of graphene which is rolled along a particular axis to form a seamless cylinder, and its electronic properties are determined by the chirality and diameter of the resulting tube. However, graphene is not the only structural motif on which a nanotube can be based; in theory, nanotubes based on a variety of 2D carbon allotropes are possible.<sup>1</sup> In the past decade, there has been a rapid expansion in the family of 2D carbon allotropes, owing to the unique chemical properties of carbon, which is able to form networks of various dimensionalities based on combinations of  $sp$ -,  $sp^2$ -, and  $sp^3$ -hybridized carbon atoms. Recently investigated 2D carbon allotropes based on  $sp$ - and  $sp^2$ -hybridized carbon include graphynes,<sup>1</sup> graphenylene,<sup>2</sup> pentahexoctite<sup>3</sup> and a host of others consisting of networks of polygons ranging from linear chains to dodecagons.<sup>4</sup>

Graphenylene has recently become the focus of several investigations<sup>2,5–7</sup> due to its unique geometry. Its structure has been characterized as highly favorable for hydrogen separation applications,<sup>6</sup> and it has been shown through density functional theory (DFT)-based simulations to be a promising anode material for lithium-ion batteries.<sup>7</sup> The unit cell of graphenylene, shown in Figure 1b, contains two six-membered carbon rings connected by a four-membered (cyclobutadiene) unit. Geometry relaxations in the framework of DFT,<sup>5,6</sup> including in the present work, have predicted three distinct bond lengths, labeled  $L_1$ ,  $L_2$ , and  $L_3$  in Figure 1b. Each six-membered ring contains two distinct alternating bond lengths, and thus a heterogeneous electron density around the ring.

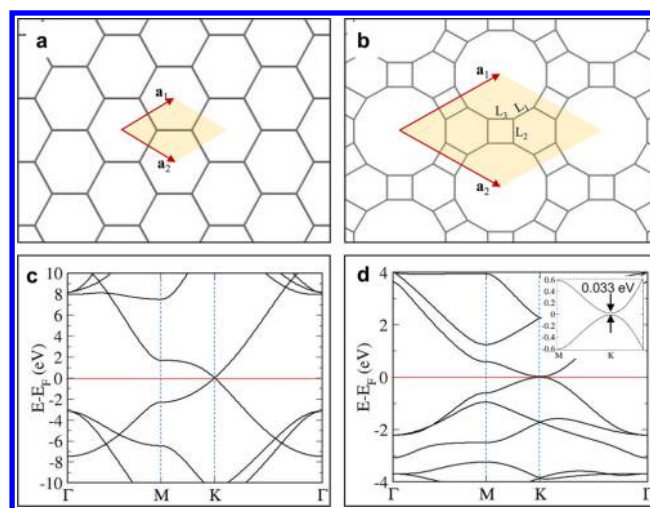


**Figure 1.** (a) 2D unit cell of graphene and (b) graphenylene.  $L_1$ ,  $L_2$ , and  $L_3$  represent the three distinct bond lengths found in graphenylene. (c) Band structure of graphene and (d) graphenylene from DFT calculations in this work. Although graphene is a known zero-gap semimetal, DFT calculations in this work predict a small, direct band gap of 0.033 eV for graphenylene. The inset in (d) shows detail of the direct band gap at the K-point conduction valley.

Molecular fragments of graphenylene have already been successfully synthesized in linear, armchair, and zigzag form,<sup>8</sup>

**Received:** August 5, 2015

**Accepted:** September 16, 2015

**Published:** September 16, 2015

although large-scale synthesis has not yet been achieved. However, Brunetto et al.<sup>5</sup> have shown through DFT-based molecular dynamics simulations that large-area graphenylene sheets could potentially be synthesized via dehydrogenation of highly ordered porous graphene, a process which results in spontaneous interconversion to graphenylene.

The electronic properties of graphenylene have been scarcely studied thus far. The band structure is of particular interest because the zero band gap of graphene gives it semimetallic character and limits its potential electronic applications. Song et al.<sup>6</sup> calculated the electronic properties of graphenylene using DFT methods with a variety of exchange-correlation functionals and reported an extremely narrow, direct band gap of 0.025 eV. As explained below (and as seen in the band structure of Figure 1d), a band gap of 0.033 eV is predicted in the present study. However, it is understood that DFT tends to significantly underestimate band gap values.<sup>9</sup> For this reason, Brunetto et al.<sup>5</sup> employed DFT-based tight-binding calculations, which predicted a direct band gap of 0.8 eV.

Nanotubes based on a graphenylene motif have so far only been briefly alluded to in terms of their geometric configuration,<sup>2</sup> but their electronic properties and exact geometry have yet to be investigated. Just as a sheet of graphene can be geometrically rolled into armchair, zigzag, and various chiral orientations, graphenylene nanotubes (GNTs) are possible. Because the unit cell of the graphenylene sheet has the same rhombic character as that of graphene, the traditional  $(n,m)$  nomenclature used to describe CNTs can be retained.

In this work, the structure and electronic properties of graphenylene nanotubes of armchair and zigzag (and a few chiral) orientations are investigated using DFT, and the results are compared to DFT-based tight binding results. One unique aspect compared to CNTs, readily seen in Figure 2, are the

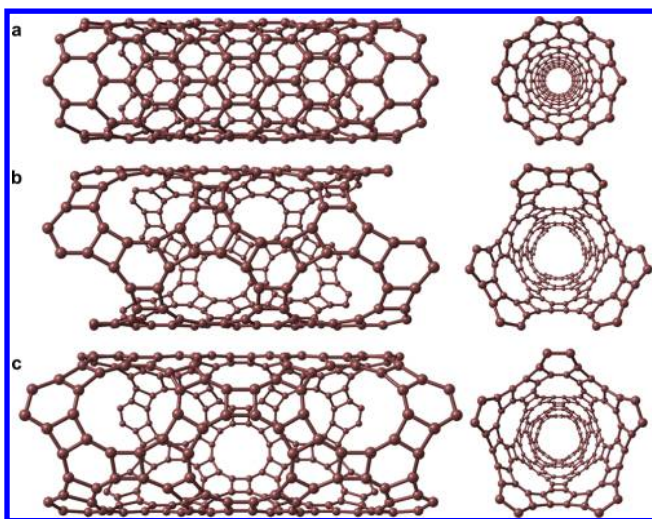


**Figure 2.** Three-dimensional views of (a) a conventional  $(n,m) = (10,0)$  CNT, (b) a  $(3,3)$  armchair GNT, and (c) a  $(5,0)$  zigzag GNT.

dodecagonal rings on the sidewalls, which form pores which may be advantageous for materials transport for applications in materials storage and electrochemical charging processes.

Graphenylene nanotubes can be geometrically constructed by rolling a slice of a 2D graphenylene sheet into a seamless cylinder, in the same way that a CNT can be considered as a rolled sheet of graphene. This allows arbitrary GNTs to be constructed by defining the chiral indices  $n$  and  $m$ . As in CNTs,

zigzag GNTs correspond to  $(n,0)$  chiral indices and armchair GNTs to  $(n,n)$  indices. A MATLAB script was written to generate the initial GNT atomic coordinates using the coordinates for 2D graphenylene and the parameters defined for CNTs, which are applicable to GNTs, such as the nanotube chiral vector  $\vec{C}_h$  and translational vector  $\vec{T}$ <sup>10</sup>

$$\vec{C}_h = n\vec{a}_1 + m\vec{a}_2 = (n,m) \quad (1)$$

$$\vec{T} = t_1\vec{a}_1 + t_2\vec{a}_2 = (t_1,t_2) \quad (2)$$

where

$$t_1 = \frac{2m + n}{\text{gcd}(2n + m, 2m + n)} \quad (3)$$

$$t_2 = -\frac{m + 2n}{\text{gcd}(2n + m, 2m + n)} \quad (4)$$

and gcd denotes greatest common divisor. Similar to CNTs, the lattice vectors are

$$\vec{a}_1 = \left( \frac{\sqrt{3}}{2}, \frac{1}{2} \right) a_0 \quad (5)$$

$$\vec{a}_2 = \left( -\frac{\sqrt{3}}{2}, \frac{1}{2} \right) a_0 \quad (6)$$

but with  $a_0$  being the translational distance between 12-membered rings, as shown in Figure 1b, rather than the distance between second-nearest neighbor carbon atoms as in CNTs.

Two approaches were used for evaluating the band structures of the GNT nanotubes. DFT calculations for the nanotubes were performed using SIESTA software package<sup>11</sup> in the generalized gradient approximation (GGA), with the variant of the Perdew–Burke–Ernzerhof (PBE) exchange-correlation functional parametrized for solids, known as PBEsol.<sup>12</sup> This functional has been used in the literature to calculate the electronic properties of 2D graphenylene<sup>6</sup> and results in improved equilibrium geometries and lattice constants, particularly for carbon nanotubes<sup>13</sup> and close-packed structures,<sup>12</sup> over the commonly used original PBE functional. Interactions of the valence electrons with the nuclei and core electrons were described through fully nonlocal Troullier–Martins pseudopotentials<sup>14</sup> obtained from the Abinit pseudopotential database. A double- $\zeta$  basis set with polarization orbitals and an energy cutoff of 50 meV was used for the valence electrons. Given the fact that periodic boundary conditions in all directions were used in the SIESTA calculations, interactions between neighboring tubes were avoided by spacing the tubes at least 15 Å apart from edge to edge. This value was determined by a systematic study on the effects of lateral spacing on electronic structure, and the energy bands were not affected at intertube spacings of >15 Å. Real-space integrations were performed on a grid with a cutoff energy of 250 Ry. The one-dimensional Brillouin zone was sampled via a Monkhorst–Pack scheme with 50 points along the single unit vector in  $k$ -space. The atomic positions were relaxed by conjugate gradient minimization until forces on the atoms were less than 0.01 eV/Å. The unit cell was relaxed together with the atomic coordinates.

Additionally, density functional-based tight-binding (DFTB) calculations were performed to predict the band structure of

GNTs using DFTB+ software package,<sup>15</sup> for the purposes of comparison with the 2D graphenylene study by Brunetto et al.<sup>5</sup> Briefly, in the DFTB method, the Kohn–Sham eigenenergies from DFT enter as diagonal elements of the Hamiltonian, and the nondiagonal matrix elements (including the overlap matrix) are calculated in a two-center approximation and stored as a table for interatomic distances up to 10 au. The Hamiltonian matrix elements are modified by a self-consistent redistribution of Mulliken charges. Atomic and diatomic contributions calculated from DFT used a PBE functional. DFTB has been used to predict the structural and electronic properties of a vast array of carbon allotropes<sup>16</sup> and has accurately predicted the opening of a band gap in graphene induced by patterned hydrogen adsorption.<sup>17</sup> The DFTB+ calculations were carried out using the optimized geometries from SIESTA calculations.

The relaxed geometry of 2D graphenylene obtained from SIESTA calculations performed in this study exhibits three distinct bond lengths. As previous studies have indicated,<sup>5,6</sup> the relaxed structure of graphenylene exhibits alternating bond lengths around each six-membered carbon ring, indicating nonuniformity of the distribution of the electron density among the corresponding  $\sigma$  bonds around the ring, unlike the case in benzene or graphene. According to our DFT calculations, the band gap of 2D graphenylene is 0.033 eV, in reasonable agreement with a previous DFT study.<sup>6</sup> The bond lengths in 2D graphenylene predicted from geometry relaxations using DFT calculations in this work are listed in Table 1, and are in

**Table 1. C–C Bond Lengths and Unit Cell Length in Graphenylene Compared with Graphene**

	graphene	graphenylene		
		L <sub>1</sub>	L <sub>2</sub>	L <sub>3</sub>
C–C bond length (Å)	1.428	1.378	1.468	1.481
$a_0$ (Å)	2.473	6.788		

good agreement with literature.<sup>5,6</sup> These calculations also predict an average pore diameter of 3.3 Å, using the method described by Song et al.,<sup>6</sup> measuring from the edge of the electron density isosurface at a value of 0.2 au.

GNTs also exhibit heterogeneous electron density distribution and, consequently, three distinct bond lengths, according to our DFT calculations. Figure 3 shows the electron density (including both  $\sigma$  and  $\pi$  contributions) of a zigzag and armchair GNT, plotted at an isovalue of 0.27  $e/\text{Å}^3$ , which clearly shows the greater density near the L<sub>1</sub> bond (not shared with the four-membered rings) compared with the L<sub>2</sub> and L<sub>3</sub> bonds (shared with the four-membered rings).

Examining the dimensions of the pores formed by the dodecagonal rings as a function of GNT diameter provides some insight into the evolution of the pores. When graphenylene is rolled into a tube, the pores are bent around the circumference of the tube, resulting in paraboloid or saddle-shaped pores. Small-diameter GNTs contain pores that are significantly narrowed in the transverse direction, whereas the pores found in large-diameter GNTs approach a circular geometry 3.3 Å in diameter. In the relaxed GNT geometry, the pores generally follow the model of a rolled sheet.

The pore diameters found in GNTs are similar in scale to the kinetic diameters of a few gases,<sup>18</sup> as seen in Figure 4a. Like 2D graphenylene, large-diameter GNTs contain pores which are larger than the kinetic diameter of H<sub>2</sub> but smaller than the kinetic diameters of O<sub>2</sub>, N<sub>2</sub>, and CO. Consequently, diffusion of

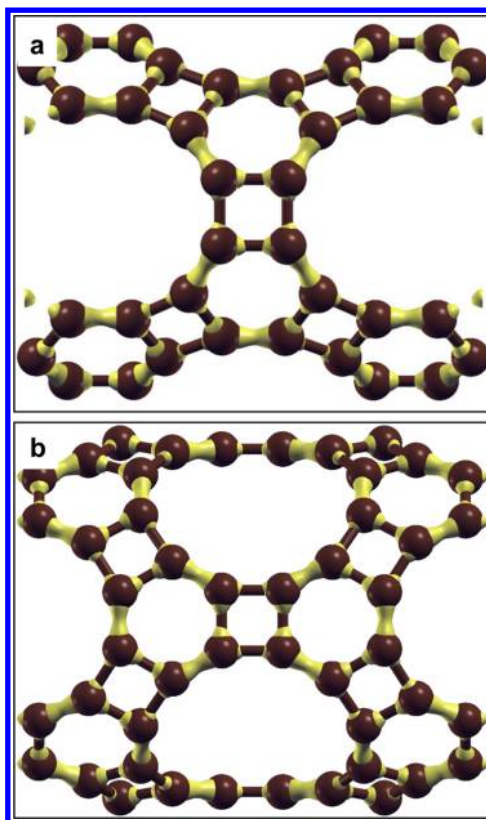


**Figure 3.** Total electron density (in yellow) of (a) a (2,2) armchair GNT and (b) a (4,0) zigzag GNT section, at an isosurface value of 0.27  $e/\text{Å}^3$ . In both cases, a higher electron density is clearly observed along the L<sub>1</sub> bond, outside of the four-membered ring, compared with the L<sub>2</sub> and L<sub>3</sub> bonds, which form the four-membered rings.

O<sub>2</sub>, N<sub>2</sub>, and CO, as well as larger gas molecules, is expected to be thermodynamically unfavorable compared with H<sub>2</sub>, making GNTs an attractive candidate for hydrogen storage and separation. Furthermore, small-diameter GNTs offer a range of pore diameters from 1.5 to 3.3 Å in the transverse direction. GNTs thus provide a wide range of selectivities for gas diffusion, dependent upon chiral index.

DFT calculations predict that graphenylene is less energetically favorable than graphene by 0.66 eV/atom, as calculated using the exchange-correlation parameters mentioned previously (GGA, PBEsol). Table 2 shows the predicted total energy per atom for a few carbon allotropes relative to graphene. A (5,5) CNT is shown as a reference for GNTs with very similar diameter.

The diameter of each GNT also has a significant and predictable effect on its total energy. Shown in Figure 4b is the curvature energy  $E_C = E_{\text{tot,GNT}} - E_{\text{tot,Graphenylene}}$  that is, the total energy per atom for each GNT relative to 2D graphenylene. Similarly to what is observed in ab initio studies of CNTs,<sup>19</sup> the curvature energy per atom increases with increasing curvature following a strict  $1/R^2$  dependence, with  $R$  being the radius of the GNT. In the commonly referenced classical theory of elasticity, the curvature energy is given by<sup>20</sup>

$$E_C = \frac{Yh^3}{24} \frac{\Omega}{R^2} = \frac{\alpha}{R^2} \quad (7)$$

where  $Y$  is the Young's modulus of the 2D sheet,  $h$  is the thickness of the tube wall, and  $\Omega$  is the atomic volume. The DFT calculations predict energies which correspond well to this

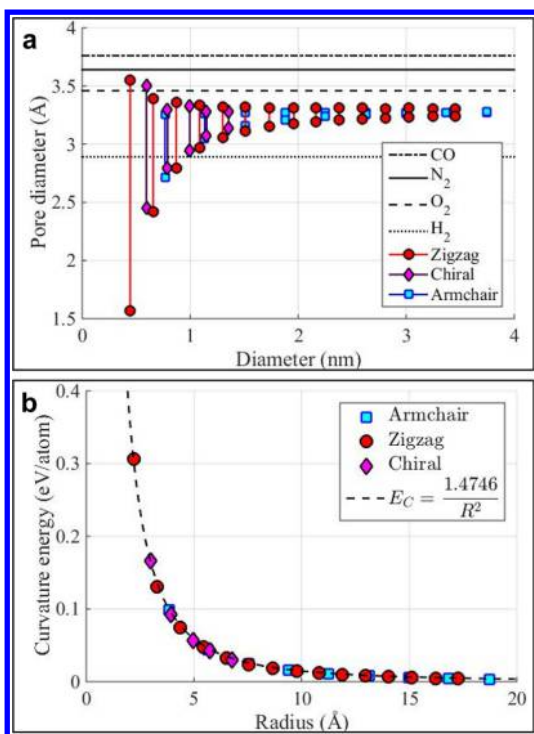


**Figure 4.** (a) Pore diameter of GNTs as a function of tube diameter, with reference to the kinetic diameters of a few gas molecules. Each line segment corresponds to a particular GNT, wherein the top data point is the diameter in the longitudinal direction and the bottom data point is the diameter in the transverse direction. (b) Curvature energy, that is, total energy per atom for graphenylene nanotubes relative to 2D graphenylene, which follows closely a  $1/R^2$  relationship, where  $R$  is the GNT tube radius.

**Table 2. Total Energy Per Atom Relative to Graphene for Various Carbon Allotropes<sup>a</sup>**

	graphene	(5,5) CNT	graphenylene	(2,2) GNT	(3,0) GNT
total energy (eV/atom)	0	0.17	0.66	0.76	0.79

<sup>a</sup>The GNTs shown here have tube radii similar to the (5,5) CNT.

relationship (with statistical  $r^2 = 0.9988$ ), where  $\alpha = 1.4746 \text{ eV} \cdot \text{\AA}^2/\text{atom}$ . If  $h$  for GNTs is considered to be the same as that of CNTs, then the ratio of the Young's moduli of 2D graphenylene and graphene<sup>19</sup> is simply  $((\alpha_{\text{graphenylene}})/(\alpha_{\text{graphene}})) = ((1.4746 \text{ eV} \cdot \text{\AA}^2/\text{atom})/(2.14 \text{ eV} \cdot \text{\AA}^2/\text{atom})) = 69\%$ . The applicability of continuum elasticity in describing the bending energy per atom in other fullerenes has been reported in the past.<sup>21</sup>

The band structures of a selection of GNTs are shown in Figure 5a and b. These bear some resemblance to those of conventional carbon nanotubes. In general, armchair  $(n,n)$  GNTs exhibit smaller (or zero) band gap values compared with their zigzag  $(n,0)$  GNT counterparts of similar diameter. The band gaps of zigzag GNTs tend to generally decrease as nanotube diameter increases, with the exception of GNTs with index  $n$  being a multiple of 3, where the band gaps are similar to those of armchair GNTs with similar diameter. This is reflected in the density of states (DOS) plots in Figure 5a, which show a small region of zero states around the Fermi level in each case except the (6,0) GNT. The similarity of these characteristics to those of CNTs, is a consequence of the similar hexagonal

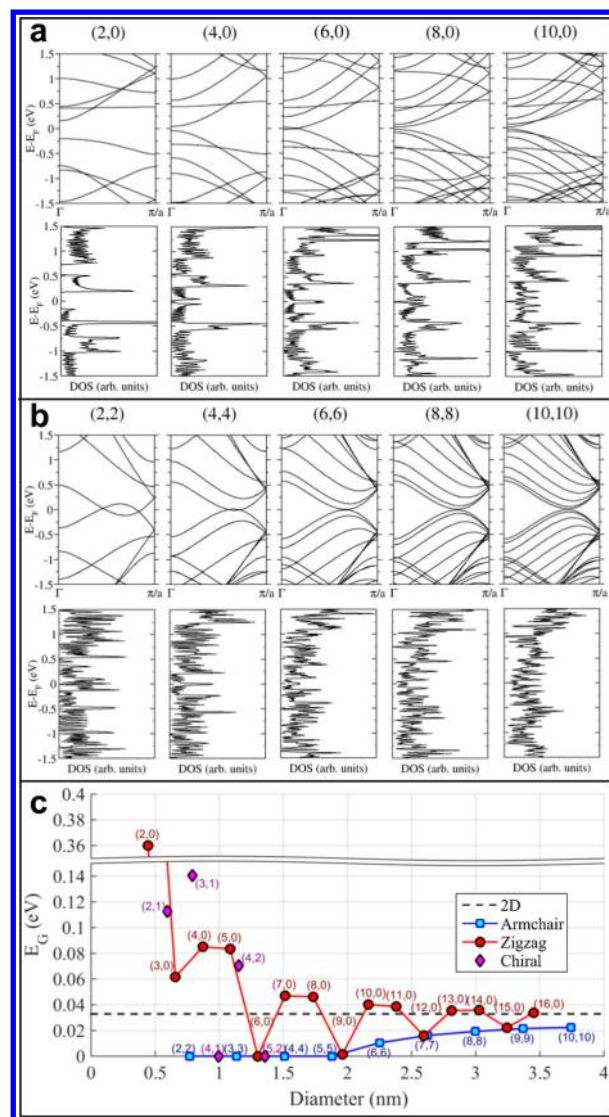


**Figure 5.** (a) Band structures and density of states plots of various zigzag and (b) armchair GNTs, according to DFT calculations. (c) Band gaps from DFT calculations of GNTs as a function of nanotube diameter, compared with 2D graphenylene. The lines are meant to help guide the eye.

Brillouin zones and location of the conduction valley at the  $K$ -point of both graphenylene and graphene. As the diameter becomes large, the limits imposed by the circumferential periodic boundary condition become less significant, and the band gap values approach the 0.033 eV value calculated for 2D graphenylene.

The DFT calculations show that the sub-bands nearest to the Fermi level in armchair GNTs cross each other in small-diameter nanotubes, as exemplified by the (2,2) and (4,4) band structures in Figure 5b. This effect disappears for large-diameter nanotubes, in which case those sub-bands become separated to form a small band gap which approaches that of 2D graphenylene. This effect is also seen in DFT calculations of small-diameter zigzag CNTs and is commonly attributed to  $\sigma^* - \pi^*$  rehybridization due to the effects of curvature of the nanotube.<sup>22,23</sup> In the DOS plot, states exist at the Fermi level for small-diameter armchair GNTs, but a small gap in the DOS opens for the largest diameters (as seen by the fact that the DOS briefly reaches the value of 0 for the case of the (10,10)

nanotube shown on Figure 5b). The overall trend in GNT band gap values can be seen in Figure 5c.

DFT-based tight-binding calculations show a similar trend in band gap values, as seen in Figure 6, with two key differences.

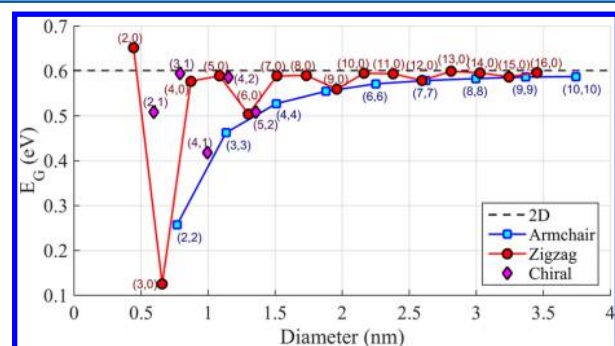


**Figure 6.** Band gaps from DFT-based tight-binding calculations of GNTs as a function of nanotube diameter, compared with 2D graphenylene. The lines are meant to help guide the eye.

First, the band gap values calculated using this method are consistently larger than those obtained using DFT calculations, as expected. Second, the decrease in band gap of armchair GNTs as diameter decreases is more severe according to these calculations, and the band gaps of small-diameter zigzag GNTs are lower than expected when compared to DFT calculations.

GNT chiralities with  $\text{mod}(n-m,3) = 0$  exhibit band gap values that distinctly follow those of armchair GNTs of similar diameter, readily observed in the (4,1), (5,2), (9,0), (12,0), and (15,0) cases in Figure 5b. The band gaps of large-diameter GNTs approach the band gap of 0.6 eV for 2D graphenylene, in comparison to 0.8 eV as predicted by Brunetto et al.,<sup>5</sup> with the difference presumably due to the exchange-correlation functional used to calculate the TB parameters.

Finally, we return to possible material-storage applications of graphenylene by briefly considering the case of lithium adsorption. In the study on 2D graphenylene by Yu,<sup>7</sup> it was shown that lithium atoms can be dispersed remarkably well on graphenylene, both in monolayer and bilayer form, and the intercalation of lithium atoms was shown to have little effect on the structure of graphenylene, meaning graphenylene-based materials would retain their mechanical properties during charging cycles in lithium-ion battery applications. GNTs offer a very unique and promising structure for lithium storage. We performed geometry relaxations in SIESTA on a (previously relaxed) (4,0) GNT with four Li atoms located just outside of the nanotube, a few angstroms radially outward from the center of the dodecagonal rings, in order to determine the equilibrium position of the Li atoms. Interestingly, the relaxed positions of the Li atoms were just inside the nanotube, as shown in Figure 7. This is in contrast to the relaxed positions of the ions near a (10,0) CNT, which are located outside of the tube. Therefore, when comparing GNTs and CNTs of the same diameter, Li intercalation may be significantly enhanced in GNTs, allowing greater storage density due to the smaller overall volume occupied by the nanotube and Li atoms together. This indicates that GNTs may be a promising material for lithium ion battery applications, and further study on lithium adsorption and diffusion is warranted.

In summary, DFT calculations predict a new family of nanotubes based on 2D graphenylene, with geometric and electronic properties similar to those of CNTs, with a few key

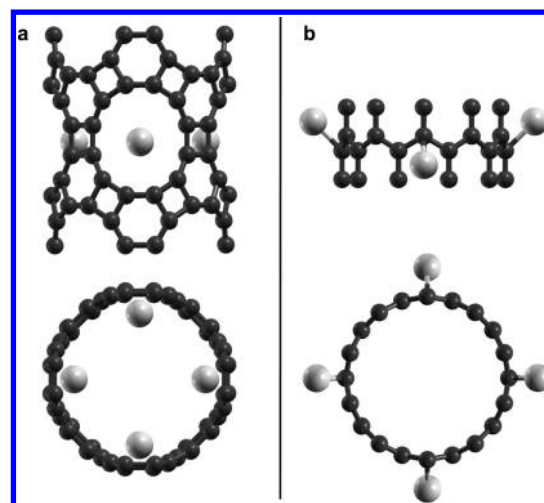


**Figure 7.** Relaxed positions of Li atoms placed outside (a) a (4,0) GNT and (b) a (10,0) CNT. The equilibrium positions of the Li atoms are located inside the GNT but outside the CNT.

differences. In terms of geometry, the dodecagonal rings found in graphenylene are bent around the circumferential axis of the tube, resulting in saddle-shaped pores. Pore diameters in the transverse direction of the tube range from 1.5 to 3.3 Å depending on chiral indices, offering a range of selectivities for materials transport applications. Concerning electronic structure, 2D graphenylene exhibits a smooth, narrow, direct band gap of 0.033 eV at the K-point of  $k$ -space, rather than a zero-gap Dirac point, according to DFT calculations. Consequently, GNTs with large diameter also exhibit a 0.033 eV band gap according to DFT calculations, although the actual band gap value is likely higher because DFT tends to underestimate band gaps. For small-diameter GNTs, zigzag GNTs exhibit larger band gap values than armchair GNTs of similar diameter, with the exception of chiral indices where  $n$  is a multiple of 3, as in the case of CNTs. In armchair GNTs of smaller diameter, as curvature increases, the sub-bands nearest to the Fermi level cross each other, which in CNT literature is attributed to  $\sigma^*-\pi^*$  rehybridization due to the effects of curvature of the nanotube. DFT-based tight-binding calculations show similar behavior of the electronic structure, only with significantly larger band gap values (0.6 eV for 2D graphenylene). Although GNTs have not yet been synthesized experimentally, their interesting properties warrant further investigation.

## ■ AUTHOR INFORMATION

### Corresponding Author

\*E-mail: [anojeh@ece.ubc.ca](mailto:anojeh@ece.ubc.ca).

### Notes

The authors declare no competing financial interest.

## ■ ACKNOWLEDGMENTS

We thank the Natural Sciences and Engineering Research Council of Canada (grant # CREATE 414110-12), the University of British Columbia and the Peter Wall Institute for Advanced Studies, for financial support. This research was enabled in part by support provided by WestGrid ([www.westgrid.ca](http://www.westgrid.ca)) and Compute Canada Calcul Canada ([www.computecanada.ca](http://www.computecanada.ca)).

## ■ REFERENCES

- (1) Coluci, V. R.; Braga, S. F.; Legoas, S. B.; Galvao, D. S.; Baughman, R. H. Families of Carbon Nanotubes: Graphyne-Based Nanotubes. *Phys. Rev. B: Condens. Matter Mater. Phys.* **2003**, *68*, 35430.
- (2) Balaban, A. T.; Vollhardt, K. P. C. Heliphenes and Related Structures. *Open Org. Chem. J.* **2011**, *5*, 117–126.
- (3) Sharma, B. R.; Manjanath, A.; Singh, A. K. Pentahexoctite: A New Two-Dimensional Allotrope of Carbon. *Sci. Rep.* **2014**, *4*, 7164.
- (4) Lu, H.; Li, S.-D. Two-Dimensional Carbon Allotropes from Graphene to Graphyne. *J. Mater. Chem. C* **2013**, *1*, 3677.
- (5) Brunetto, G.; Autreto, P. A. S.; Machado, L. D.; Santos, B. I.; dos Santos, R. P. B.; Galvão, D. S. Nonzero Gap Two-Dimensional Carbon Allotrope from Porous Graphene. *J. Phys. Chem. C* **2012**, *116*, 12810–12813.
- (6) Song, Q.; Wang, B.; Deng, K.; Feng, X.; Wagner, M.; Gale, J. D.; Müllen, K.; Zhi, L. Graphenylene, a Unique Two-Dimensional Carbon Network with Nondelocalized Cyclohexane Units. *J. Mater. Chem. C* **2013**, *1*, 38–41.
- (7) Yu, Y.-X. Graphenylene: A Promising Anode Material for Lithium-Ion Batteries. *J. Mater. Chem. A* **2013**, *1*, 13559–13566.
- (8) Schulman, J. M.; Disch, R. L. A Theoretical Study of Large Planar [N]Phenylenes. *J. Phys. Chem. A* **2007**, *111*, 10010–10014.
- (9) Sholl, D.; Steckel, J. A. *Density Functional Theory: A Practical Introduction*; Wiley-Interscience: New York, 2009.
- (10) Saito, R.; Dresselhaus, G.; Dresselhaus, M. *Physical Properties of Carbon Nanotubes*; Imperial College Press: London, 1998.
- (11) Soler, J. M.; Artacho, E.; Gale, J. D.; Garcia, A.; Junquera, J.; Ordejón, P.; Sánchez-Portal, D. The SIESTA Method for Ab Initio Order-N Materials Simulation. *J. Phys.: Condens. Matter* **2002**, *14*, 2745.
- (12) Perdew, J. P.; Burke, K.; Ernzerhof, M. Restoring The Density-Gradient Expansion for Exchange in Solids and Surfaces. *Phys. Rev. Lett.* **2008**, *100*, 136406.
- (13) Demichelis, R.; Noël, Y.; D'Arco, P.; Rérat, M.; Zicovich-Wilson, C.; Dovesi, R. Properties of Carbon Nanotubes: An Ab Initio Study Using Large Gaussian Basis Sets and Various DFT Functionals. *J. Phys. Chem. C* **2011**, *115*, 8876–8885.
- (14) Troullier, N.; Martins, J. L. Efficient Pseudopotentials for Plane-Wave Calculations. *Phys. Rev. B: Condens. Matter Mater. Phys.* **1991**, *43*, 1993–2006.
- (15) Porezag, D.; Frauenheim, T.; Kohler, T. K.; Seifert, G.; Kaschner, R. Construction of Tight-Binding-Like Potentials on the Basis of Density-Functional Theory: Application to Carbon. *Phys. Rev. B: Condens. Matter Mater. Phys.* **1995**, *51*, 12947.
- (16) Diudea, M. V.; Szefer, B.; Nagy, C. L.; Bende, A. Exotic Allotropes of Carbon. In *Exotic Properties of Carbon Nanomatter*; Springer: Netherlands, 2015; pp 185–201.
- (17) Balog, R.; Jørgensen, B.; Nilsoon, L.; Andersen, M.; Rienks, E.; Bianchi, M.; Fanetti, M.; Lægsgaard, E.; Baraldi, A.; Lizzit, S.; et al. Bandgap Opening in Graphene Induced by Patterned Hydrogen Adsorption. *Nat. Mater.* **2010**, *9*, 315–319.
- (18) Matteucci, S.; Yampolskii, Y.; Freeman, B. D.; Pinnau, I. Transport of Gases and Vapors in Glassy and Rubbery Polymers. *Materials Science of Membranes for Gas and Vapor Separation*; John Wiley & Sons, Ltd: Chichester, U.K., 2006; pp 1–47.
- (19) Gülseren, O.; Yuldirim, T.; Ciraci, S. Systematic Ab Initio Study of Curvature Effects in Carbon Nanotubes. *Phys. Rev. B: Condens. Matter Mater. Phys.* **2002**, *65*, 153405.
- (20) Robertson, D. H.; Brenner, D. W.; Mintmire, J. W. Energetics of Nanoscale Graphitic Tubules. *Phys. Rev. B: Condens. Matter Mater. Phys.* **1992**, *45*, 125492.
- (21) Tomanek, D.; Zhong, W.; Krastev, E. Stability of Multishell Fullerenes. *Phys. Rev. B: Condens. Matter Mater. Phys.* **1993**, *48*, 15461.
- (22) Blase, X.; Benedict, L. X.; Shirley, E. L.; Louie, S. G. Hybridization Effects and Metallicity in Small Radius Carbon Nanotubes. *Phys. Rev. Lett.* **1994**, *72*, 1878.
- (23) Matsuda, Y.; Tahir-Kheli, J.; Goddard, W. A. Definitive Band Gaps for Single-Wall Carbon Nanotubes. *J. Phys. Chem. Lett.* **2010**, *1*, 2946–2950.